Chapter 7

Study of Molecular Interaction of SnS Nanoparticles with Bovine Serum Albumin

Nanoscience is a significant field in the purpose of therapeutic and pharmaceutical diagnostics. There has been a growing attention in the study of binding between biomolecules with nanoparticles. Tin sulfide is an important IV–VI semiconductor and hugely applied in the area of optoelectronics as well as biomedicine [231,284]. One of the important issues is the detection of the character of protein-nanoparticle interactions and the favored of binding sites in functional characterization of biomolecules regarding their physiological responses. The interaction and the development of bioconjugate of Bovine Serum Albumin (BSA) and Tin Sulfide (SnS) nanoparticles (NPs) are studied using optical spectroscopic measurements. Optical absorption and fluorescence spectra demonstrate that a spontaneous binding process happened between BSA and SnS NPs. A minute red shift of the optical absorption peak of Albumin (BSA) is noticed due to interaction of Albumin and SnS NPs. The emission spectra of Bovine Serum Albumin (BSA) are quenched with the addition of SnS NPs. Photo luminescent semiconducting nanoparticles like SnS NPs have been connected with biocojugates molecules for example peptides, proteins etc. The SnS@BSA bioconjugate have been applied in biology based medical fields [285-286] owing to their limited properties controlled effects as compared with those of the consequent bulk materials. Photo luminescent SnS NPs have been employed the bio-imaging or bio-labelling [287-288]. The configuration of the nanoparticles-protein conjugates supplies important information about the conformational changes of protein model happening at the protein-NPs interface. The binding of nanoparticles with protein have been analyzed using different experimental

techniques such as liquid chromatography (LC), dynamic light scattering (DLS), atomic force microscopy (AFM), circular dichroism spectroscopy (CDS) as well as fluorescence spectroscopy measurements [289-290]. The study of the binding of protein-NPS bioconjugate will give information on what happens at molecular level protein-NPS interface. Whenever NPs enter the physiological fluid systems they will interact with the surrounding of protein molecules. Protein molecules can interact to the semiconducting NPs strongly and a dynamic proteins layer is produced on the NPs surfaces. This bio conjugated structure is recognized as "NPs-protein corona" [291-292]. As the NPs-protein corona plays a significant role for the bio-nano interface [293], so it is important of the development process from the discrete protein-NPs conjugates to NP's protein corona [294]. Bovine serum albumin (BSA) has been one of the most widely studied protein model due to its structural homology with human serum albumin (HSA).

Tin Sulfide (SnS) nanoparticles (NPs) have been synthesized by simple solvothermal route. The XRD pattern of the grown samples indicates the orthorhombic crystal structure of SnS. TEM images shows the sizes of grown samples are within the range 4 nm to 6 nm. We have studied the formation of bioconjugate of bovine serum albumin (BSA) with SnS NPs with the help of the TEM images and the fluorescence quenching measurements in connection with the Stern-Volmer and Hill equations. A spontaneous binding process is observed between BSA and SnS NPs which were confirmed by UV–Vis absorption and fluorescence spectra. PL spectra indicate a red shift of SnS NPs with respect to pure BSA. The PL decay lifetime of BSA in the presence of SnS NPs with highest concentration signifies the quenching process follows static mechanism. Some binding parameters like Stern–Volmer quenching constant, binding constant as well as Hill coefficient were also determined.

7. 1. Experimental section

7.1.1. Sample preparation

Solvothermal route was followed to prepare good quality SnS NPs. In brief, 1.13 gm of tin chloride and 0.39 gm of sodium sulfide were mixed individually in 20 ml and 30 ml ethylene glycol respectively through magnetic stirring. After that, dispersed solution of tin chloride was added drop wise into the sodium sulfide dispersed solution under stirring condition. The obtained precipitate was put into a Teflon-lined stainless steel autoclave. Then the autoclave was placed in a furnace and heated up to 180 ^{0}C for 18 h and then the solution was allowed to cool down to normal temperature naturally. The obtained precipitate was centrifuged and washed with deionised water for many times and finally dried at 50 ^{0}C for 72 hrs. The as synthesized SnS NPs was dispersed in Millipore water for 25 mins through ultrasonification. The concentration of SnS NPs was varied from 0.001 mg/ml to 0.05 mg/ml. The mixed solution of protein (BSA) and SnS NPs were prepared by mixing 0.1 mg/ml of protein (BSA) with SnS NPs which was ranging from 0.001 mg/ml to 0.05 mg/ml with appropriate ratio.

7.1.2. Sample characterizaion

The XRD pattern of as prepared powder sample (SnS NPs) was recorded using X-ray diffractometer by Bruker Axs D2 phaser SSD160 with Cu-kα radiation of λ=1.5405Å for 2θ value in the range between 10° to 70°. The prepared SnS NPs have been dispersed clearly in the water through ultrasonification for 20 minutes. For microstructural properties study, a little drop of the dispersed SnS NPs was taken on a thin carbon coated copper grid and dried for some time. The transmission electron microscopy (TEM) of as prepared samples was studied by JEOL JEM200 with an operating voltage at 200KV. The selected area electron diffraction (SAED) pattern of as prepared samples was also studied. Time-Correlated Single Photon Counting (TCSPC) of as prepared pure sample as well as SnS@BSA bioconjugate

have been performed by Delta flex-01-DD. Optical absorption spectra of the samples dispersed in water were measured by Shimadzu-Pharmaspec-1700 UV-VIS spectrophotometer in the optical range of 230nm-700nm at room temperature. Photoluminescence spectra (PL) of the dispersed samples were recorded by Perkin Elmer LS55 Fluorescence Spectrometer.

7. 2. Results and discussion

7.2.1. Study of X-ray diffraction (XRD)

The X-ray diffraction pattern of as prepared SnS nanopowder was recorded using X-ray diffractometer by Bruker Axs D2 phaser SSD160 with Cu-kα radiation (λ=1.5405Å) in the range of 10° to 70° is depicted in fig. 7.1. From the diffraction pattern, it is seen that all the diffraction planes indexed as [120], [101], [111], [040], [101], [131], [115] and [125] are situated for 2θ values at 26.70^0, 30.14^0, 31.09^0, 32.14^0, 34.28^0, 38.07^0, 52.16^0 and 64.61^0 respectively.

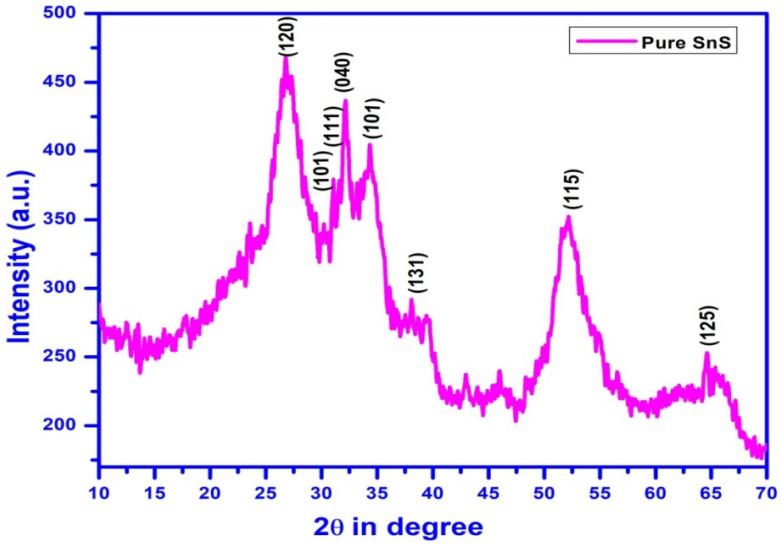

Fig. 7.1. The XRD pattern of pure SnS NPs

Therefore, these diffraction planes are perfectly matched with the orthorhombic structure of phase of SnS nanocrystals (JCPDS card no: 39-0354). The average particle diameter of SnS NPs has been estimated with the help of Debye Scherer formula:

$$P = \frac{0.9\,\lambda}{\beta \cos\theta} \qquad (7.1)$$

Where, λ is the wavelength of X-rays which is 1.5405Å, $\beta_{1/2}$ is the full width half maximum (FWHM), θ is the Bragg angle. The calculated average particle diameter of the as prepared SnS NPs was close to 2.7 nm.

7.2.2. Transmission electron microscopy (TEM) study

The high-resolution transmission electron microscope (HRTEM) was used to study the morphology properties of as prepared samples. Fig. 7.2 (a) gives the HRTEM picture of the pure SnS nanostructure with average grain size of 5.50 nm. It is observed that the SnS NPs are distributed with better uniformly. The SAED pattern of the pure SnS is depicted in fig. 7.2 (b) which signifies the crystalline behaviour of pure SnS NPs. The HRTEM image as well as SAED pattern of the BSA-SnS NPs complex is also displayed in figure 7.2(c) and 7.3(d) respectively.

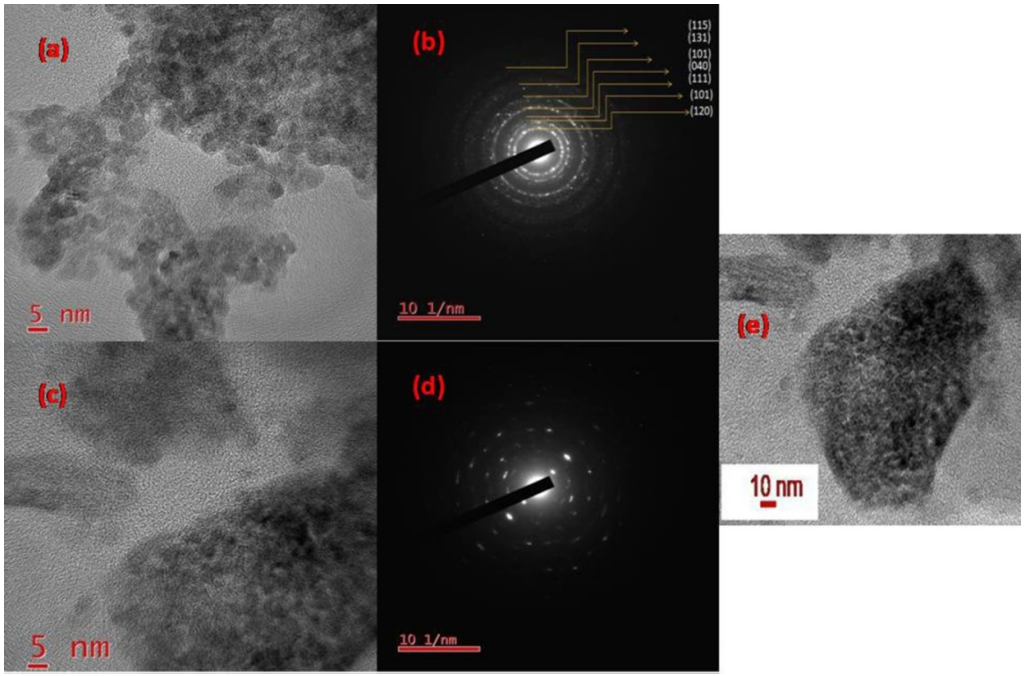

Fig 7.2. (a) HRTEM of pure SnS NPs; (b) SAED pattern of pure SnS NPs; (c) HRTEM of SnS-BSA conjugate; (d) SAED of SnS-BSA conjugate (e) HRTEM of SnS-BSA conjugate with higher resolution.

The HRTEM images demonstrate that SnS nanoparticles (NPs) facilitate the aggregation of BSA into nano fibrillar aggregates. Therefore, it is confirmed that the SnS NPs is capped by the BSA protein model is shown in figure 7.2(c). The figure 7.2(e) exhibited the HRTEM image of nano-bio complex with higher resolution.

7.2.3. TCSPC study

Time-Correlated Single Photon Counting (TCSPC) measurement is a helpful study to understand the type of the interaction between the colloidal semiconductor nanoparticles (NPs) and the model of protein system. Generally, the TCSPC measurement is the best method to analyse the process of static and dynamic quenching. In the recent work we have discussed the effect of SnS NPs on the fluorescence decay lifetime of BSA. The PL decay life time of the carriers have been estimated from the following formula

$$\tau_{av} = \sum \frac{\alpha_i \tau_i}{\alpha_i} \qquad (7.2)$$

Where $\tau's$ are the decay components and α's are the respective amplitudes of life time components. The PL decay life time of the pure SnS is shown in fig 3. On the other hand, the PL decay life time of pure BSA and BSA-SnS complex with high concentration as well as low concentration is also depicted in fig. 7.3. It is observed that the PL decay life time of pure BSA is about 6.64 ns, and then with the first addition of SnS NPs (low concentration) changed the decay curve and shows the PL decay life time is about 6.34 ns. However, with the further rise of the concentration of SnS NPs the PL decay lifetime of BSA (6.31 ns) remains almost unchanged. The PL decay life time for pure BSA followed single exponential decay whereas for BSA-SnS complex it follows double exponential decay fashion. Therefore, there is no change in the PL decay lifetime of BSA in the presence of SnS NPs with highest concentration signifies that the quenching process follows static mechanism. The decrease in

PL decay life time of BSA-SnS complex is probably due to the increased in transfer energy efficiency [295].

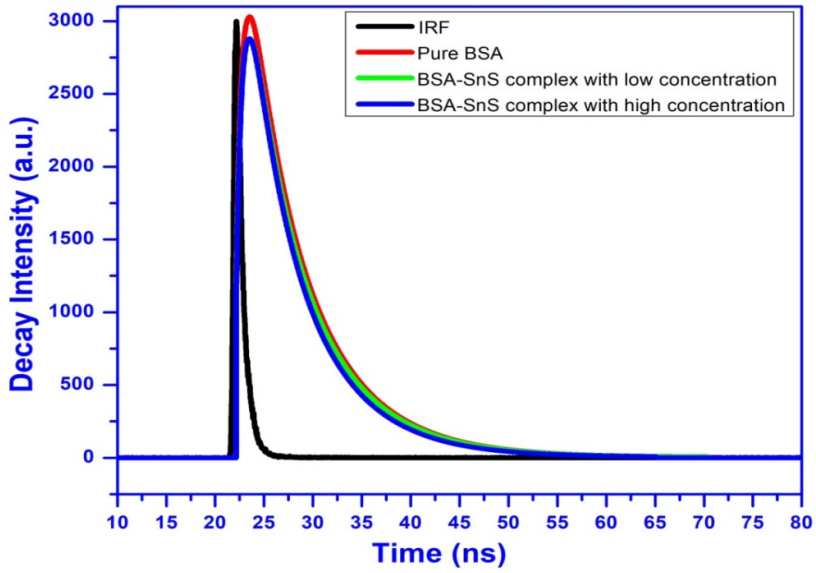

Fig. 7.3. PL decay life time of the pure SnS and BSA-SnS complex

7.2.4. UV-vis spectroscopy study

The optical absorption spectrum of as prepared pure SnS NPs is depicted in fig. 7.4(b) whereas the optical absorption spectra of BSA–SnS complex are shown in fig. 7.4(a). The BSA displayed an absorption peak situated at 279 nm which is due to the presence of (Π-Π* transition) aromatic amino acid residues [174]. The presented UV-vis absorption spectra (shown in Figs. 7.4a) demonstrate the binding effect of SnS NPs with the model of BSA. The fig. 7.4(a) also showed that the optical absorbance coefficient increases with the increase of concentration of SnS NPs. The enhancement of the absorbance intensity of bovine serum albumin (BSA) in the presence of SnS NPs possibly due to interaction of BSA with SnS NPs as well as the development of the ground state complex [296].

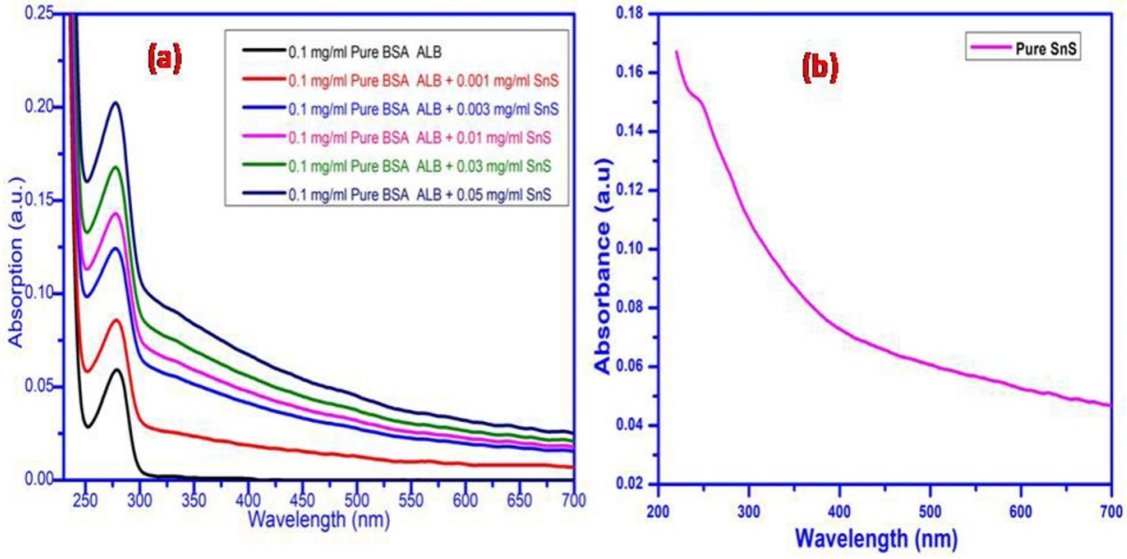

Fig. 7.4. Absorption spectra of (a) pure BSA with 0.1mg/ml , and BSA – SnS NPs complex with 0.1mg/ml of BSA and 0.001, 0.003, 0.01 0.03, 0.05 mg/ml of SnS NPs, (b) Pure SnS NPs.

7.2.5. Fluorescence quenching study

Fluorescence spectroscopy is an important technique to study of the deformation or conformational changes of protein molecules. It is also responsible for the BSA-SnS NPs complex formation. Here, we have employed the fluorescence quenching system [297-298] to analysis binding kinetics of the interaction of BSA-SnS complex. Fig 7.5(a) gives the emission spectroscopic image of pure SnS NPs. The SnS NPs-BSA binding kinetics symmetry has been investigated by fluorescence quenching study. The emission spectra of pure BSA as well as BSA-SnS NPs complex are depicted in fig 7.5(b). A quenching of the intensity of the emission spectra is observed with the addition of SnS NPs with different concentrations [299-300]. The observed fluorescence emission quenching may be due to the transfer of energy taking place between BSA and SnS NPs. The quenching phenomenon arises via the adsorption as well as the interaction of the BSA residues available at the metallic face of the SnS NPs. The quenching of emission spectra can be explained by the Stern-Volmer equation

$$F_0/F=1+K_{SV}\,[C] \qquad (7.3)$$

Where, F_0 is fluorescence intensities in the absence of quencher and F is the fluorescence intensities in the presence of quencher. K_{SV} is the Stern-Volmer quenching constant. [C] is the concentration of the quencher. The plot of F_0/F with the concentration of the quencher [C] in mg/ml has been shown in fig. 7.5(c). The Stern-Volmer quenching constant (K_{SV}), measure of the quenching efficiency was calculated and it was found to be 11.1762 ml/mg. The relation between the fluorescence intensity and concentration of the quencher is described by the following equation is given by,

$$ln\frac{(F_0 - F)}{F} = lnK_b + n\ln[C] \qquad (7.4)$$

Where, K_b is the binding constant and n is the Hill coefficient. The Hill equation can be employed to investigate the quenching information significantly. A plot of $\ln[(F_0\text{-}F)/F]$ vs log[C] have been used (fig. 7.5d) to calculate the binding constant (K_b) and Hill coefficient (n).

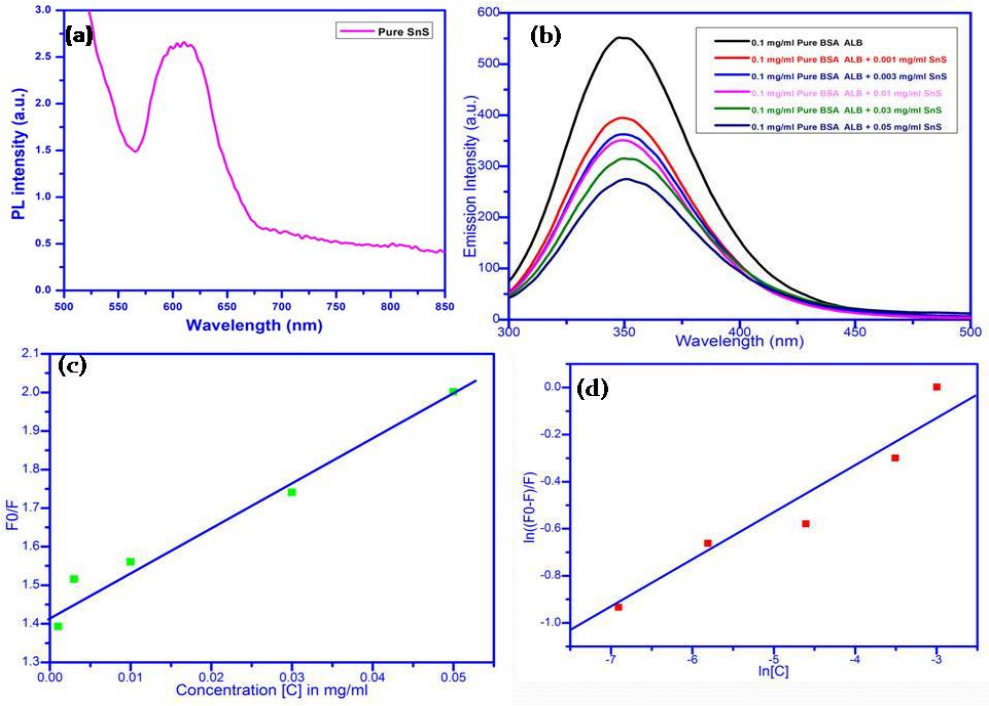

Fig. 7.5. Emission spectra of (a) pure SnS NPs ; (b) pure BSA with 0.1mg/ml , and BSA – SnS NPs complex with 0.1mg/ml of BSA and 0.001, 0.003, 0.01 0.03, 0.05 mg/ml of SnS NPs ; (c) F_0/F vs C (mg/ml); (d) ln $[(F_0\text{-}F)/F]$ vs ln[C].

The binding constant (K_b) as well as the Hill coefficient (n) between BSA and SnS NPs were found to be 1.68 ml/mg and 0.21 respectively. Besides, the Hill coefficient (n) illustrates the degree of cooperativity in ligand binding to a surface. Our results show that a negative cooperative phenomenon happens. According to our result, the association energy for each particle gradually reduces with more adsorption of BSA molecules. Therefore, the interaction of BSA – SnS NPs complex is weak.

7.3. Conclusion

We have grown and characterized tin sulfide (SnS) nanoparicles successfully by solvothermal route. The average particle diameter of pure SnS NPs has been estimated from TEM micrograph and it was found to be approximately 5.50 nm. The binding of BSA - SnS NPs complex were studied through structural and optical study. The PL decay lifetime of BSA in the presence of SnS NPs with highest concentration signifies that the quenching process follows static mechanism. The fluorescence quenching of the SnS NPs-BSA system showed a weak interaction. Also, the binding between SnS nanoparicles with BSA showed a negative cooperative phenomenon. The HRTEM images demonstrate that SnS nanoparticles (NPs) facilitate the aggregation of BSA into nano fibrillar aggregates. Therefore, it is confirmed that the SnS NPs is capped by the BSA protein model. This also indicates the interaction of the protein (BSA) model with SnS nanoparicles. This study provides a chance for potential applications in the field of biotechnology.